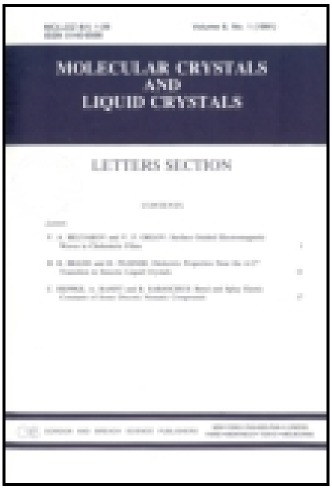

Molecular Crystals and Liquid Crystals
Publication details, including instructions for authors and subscription information:
http://www.tandfonline.com/loi/gmcl20

OLED Light Outcoupling Enhancement by Extracting Surface Plasmon Polariton Energy

Hyun-Jun Cho[a] & Ho-Nyeon Lee[b]

[a] Department of Electric & Robotics Engineering, Soonchunhyang University, Asan, Korea

[b] Department of Display and Electronic Information Engineering, Soonchunhyang University, Asan, Korea

Published online: 06 Dec 2014.

To cite this article: Hyun-Jun Cho & Ho-Nyeon Lee (2014) OLED Light Outcoupling Enhancement by Extracting Surface Plasmon Polariton Energy, Molecular Crystals and Liquid Crystals, 601:1, 159-164, DOI: 10.1080/15421406.2014.940795

To link to this article: http://dx.doi.org/10.1080/15421406.2014.940795

Mol. Cryst. Liq. Cryst., Vol. 601: pp. 159–164, 2014

ISSN: 1542-1406 print/1563-5287 online
DOI: 10.1080/15421406.2014.940795

Taylor & Francis
Taylor & Francis Group

OLED Light Outcoupling Enhancement by Extracting Surface Plasmon Polariton Energy

HYUN-JUN CHO[1] AND HO-NYEON LEE[2,*]

[1]Department of Electric & Robotics Engineering, Soonchunhyang University, Asan, Korea
[2]Department of Display and Electronic Information Engineering, Soonchunhyang University, Asan, Korea

The extraction method of surface plasmon polariton (SPP) energy was investigated to assess its ability to improve the outcoupling efficiency of organic light-emitting diodes (OLEDs). A multi-cathode OLED (MC-OLED) structure was used; this structure was composed of a semitransparent cathode (Ag), a high refractive index dielectric layer (WO_3), and a reflector (Ag). The dependence of the current efficiency of MC-OLEDs on the thicknesses of the Ag cathode and the WO_3 dielectric was examined, and optimal thicknesses were identified. Current efficiency can be increased by 20% more than conventional OLEDs by using a 50-nm Ag cathode and a 100-nm WO_3 dielectric.

Keywords Light-emitting diode; multi-cathode; outcoupling; surface plasmon polariton (SPP)

Introduction

Organic light-emitting diodes (OLEDs) are becoming an important area of display technology due to the active commercialization of active-matrix OLEDs (AMOLEDs). AMOLEDs have been commercialized in small products such as displays for smartphones, smart pads, and digital cameras. Recently, flat panel display (FPD) industries have started to expand their business to large OLED televisions. Power efficiency is a key factor in this expansion, so improving the power efficiency of OLEDs is currently an important research issue. The efficiency of OLEDs is determined by the product of the internal quantum and outcoupling efficiencies. While internal efficiency was much improved, external OLED efficiency remains unsatisfactory because of loss during the light outcoupling process. Therefore, improvement of the outcoupling efficiency is an urgent research issue. In general, about 20% of internally generated light escapes from OLED devices [1, 2]. Loss due to waveguide and SPP modes causes this low outcoupling efficiency. Various methods have been proposed for extracting the waveguide mode energy to outside, including microcavities [3, 4], photonic crystals [5, 6], microlens arrays [7, 8], surface modification [9], and light scattering layers [10]. However, a focus on waveguide modes is insufficient to improve

*Address correspondence to Prof. Ho-Nyeon Lee Department of Display and Electronic Information Engineering Soonchunhyang University, Asan 336-745, Korea (ROK). Tel.: (+82)10-4752-1248; Fax: (+82)41-530-1548. E-mail: hnlee@sch.ac.kr

Color versions of one or more of the figures in the article can be found online at www.tandfonline.com/gmcl.

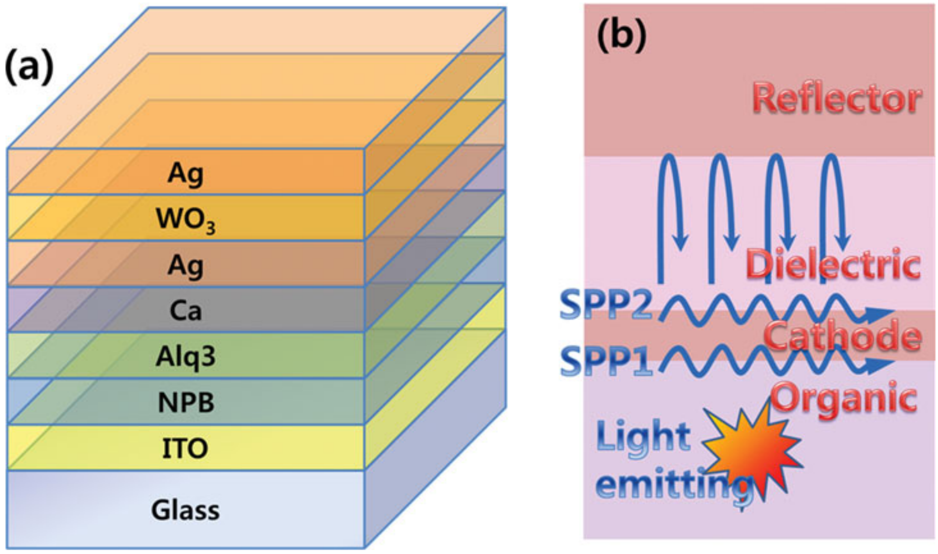

Figure 1. (a) Schematic of the device structure. (b) Illustration of the principle of light extraction from the SPP modes.

light extraction efficiency, because SPP modes trap a considerable portion of the generated light. Some researchers have reported light extraction from SPP modes [11–13]; most of this kind of research involved methods using wavelength-scale patterns to break the SPP modes. Despite the increased outcoupling efficiency, the fabrication process of the wavelength-scale patterns is too expensive for use in the mass production of FPDs. Recently, a SPP extraction method using a multi-cathode structure without micro-patterning was proposed [14]. Multi-cathode OLEDs (MC-OLEDs) have a structure involving a sequential stack of a semi-transparent cathode layer, a dielectric layer, and a reflecting layer. The feasibility of this method for improving outcoupling efficiency has been assessed, but the device physics are not clearly understood, and the method has considerable room for improvement, specifically obtaining highly efficient OLEDs.

This work investigated the dependence of outcoupling efficiency on the SPP extraction structure of MC-OLEDs. Variations in current efficiency according to the thickness of the cathode and the dielectric were measured. The results revealed that extracting light from the SPP modes can increase the current efficiency of OLEDs more than 20%.

Experiments

Figure 1(a) presents a schematic of the experimental device structure, which was glass substrate/indium tin oxide (ITO) (150 nm)/N,N′-bis(naphthalen-1-yl)-N,N′-bis(phenyl)-benzidine (NPB) (20 nm)/tris(8-hydroxy-quinolinato)aluminum (Alq_3) (60 nm)/Ca (5 nm)/Ag cathode/WO_3/Ag (100 nm). A 0.5t glass was used as the substrate, and plasma-beam-deposited ITO with a sheet resistance of 10 Ω/sq was used as an anode electrode. Anodes were patterned using a photolithography and a wet etching method. After the anode patterning, oxygen-plasma treatment was conducted using inductively coupled plasma equipment. NPB hole transporting layer (HTL), Alq_3 light emitting and electron transporting layer (EL-ETL), Ca electron injection layer (EIL), Ag cathode, WO_3 dielectric, and Ag reflector were then deposited sequentially using a thermal evaporation method at a pressure

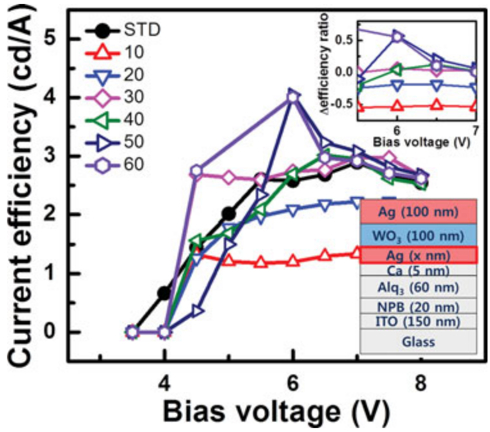

Figure 2. Current efficiency of OLEDs as a function of bias voltage according to the thickness of the Ag cathode. The upper inset presents the Δcurrent efficiency according to the cathode thickness, and the lower inset presents a schematic of the stacked structure.

of 10^{-6} Torr. The patterning was conducted using a shadow mask method. Next, the OLED device was encapsulated using a glass lid in a nitrogen environment. After the encapsulation process, the current-voltage-luminance characteristics were measured in a dark shielding box.

Results and Discussion

Figure 1(b) illustrates the principle of light extraction from SPP modes of MC-OLEDs. Light generated in an organic layer can be trapped into SPP1 modes at the cathode/organic interface by near-field coupling [15]. The light energy of the SPP1 modes can be extracted via two different paths: first, it can be transferred to SPP2 [11, 12, 16] and then extracted into the dielectric. Second, it can be transferred directly to radiation modes in the upper dielectric [15]. To activate these transfer mechanisms, the refractive index of the dielectric layer must be equal to or higher than that of the organic layers. The light energy in the dielectric can be reflected and directed to the bottom by the Ag reflector. Following this sequence, the light energy in the SPP1 modes can be extracted outside, so the external efficiency can be increased.

Figure 2 presents OLED current efficiency as a function of bias voltage, according to the thickness of the Ag cathode. For comparison, the figure also presents the results from a standard (STD) OLED, which was fabricated using a conventional bottom emission structure. Its stacked layers below the cathode were the same as the MC-OLEDs used in this research. The stacked structure of the standard OLED was glass substrate/ITO anode (150 nm)/NPB HTL (20 nm)/Alq_3 EL-ETL (60 nm)/Ca EIL (5 nm)/Ag cathode (150 nm). The stacked structure of other MC-OLEDs was glass substrate/ITO anode (150 nm)/ NPB HTL (20 nm)/Alq_3 EL-ETL (60 nm)/Ca EIL (5 nm)/Ag cathode (x nm)/WO_3 dielectric (100 nm)/Ag reflector (100 nm). The lower inset of the figure presents a schematic diagram of the stacked structure of MC-OLEDs. The thickness of the Ag cathode was varied from 10 to 60 nm. Thin Ag films (10 nm, 20 nm) were not efficient at improving the device efficiency, but a noticeable improvement in current efficiency was observed for the thicker Ag film cases. Average current efficiency values of devices are shown in Table 1; these were averaged using measured data for bias voltage of 6 to 7 V. The upper inset of the

Table 1. Current efficiency according to the Ag cathode thickness

Cathode thickness (nm)	10	20	30	40	50	60
Current efficiency (cd/A)	1.28	2.16	2.83	2.89	3.45	3.30

figure presents the Δcurrent efficiency according to the cathode thickness, calculated as:

$$\Delta \text{ current efficiency} = \frac{(\text{current efficiency of an MC-OLED}) - (\text{current efficiency of the standard OLED})}{\text{current efficiency of the standard OLED}}. \quad (1)$$

Current efficiency increased with the thickness of the Ag cathode up to 50 nm, and then decreased. The 50 nm Ag cathode condition yielded a Δcurrent efficiency of more than 20%. To transfer the light energy of SPP modes at the front interface (organic/cathode interface) into the dielectric, the light energy had to go through the Ag cathode layer. The light takes the form of an evanescent field in a metal layer (Ag cathode). Normally, evanescent fields in a metal decrease exponentially as the field progresses into the metal layer, so a thicker metal film decreases the coupling efficiency between the fields of each side. However, near the SPP resonance frequency, the field intensity in an Ag film can increase as the field progresses up to a certain thickness [17, 18]. This phenomenon could explain our results for the dependence of current efficiency on Ag cathode thickness.

Figure 3 presents the current efficiency of OLEDs as a function of bias voltage, according to the thickness of the WO_3 dielectric. The standard (STD) OLED had a structure identical to that of the standard OLED shown in Fig. 2. The structure of other MC-OLEDs in Fig. 3 were glass substrate/ITO anode (150 nm)/NPB HTL (20 nm)/Alq_3 EL-ETL (60 nm)/Ca EIL (5 nm)/Ag cathode (50 nm)/WO_3 dielecric (x nm)/Ag reflector (100 nm). The thickness of the Ag cathode was fixed at 50 nm, based on the results shown in Fig. 2. The upper inset in Fig. 3 presents a schematic of the stacked structure. The thickness of

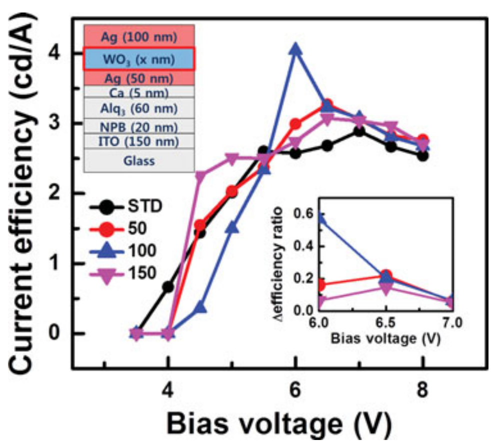

Figure 3. Current efficiency of OLEDs as a function of bias voltage, according to the thickness of the WO_3 dielectric. The upper inset presents a schematic of the stacked structure, and the lower inset presents the Δcurrent efficiency according to the WO_3 thickness.

Table 2. Current efficiency according to the WO_3 dielectric thickness

Dielectric thickness (nm)	50	100	150
Current efficiency (cd/A)	3.11	3.45	2.95

the WO_3 dielectric was varied from 50 to 150 nm. The current efficiency was not severely dependent on the dielectric thickness, but the 100 nm WO_3 condition was more efficient than the 50 nm and 150 nm WO_3 conditions, considering the overall operation range. Average current efficiency values of devices are shown in Table 2; these were averaged using measured data for bias voltage of 6 to 7 V. The lower inset in Fig. 3 presents the Δcurrent efficiency according to the WO_3 thickness. The refractive index of WO_3 was approximately 2.0 [19]. The SPP wave vector at the metal surface faced with the lower refractive index dielectric can be located in the radiative region of the dispersion relation of the metal surface faced with the higher refractive index dielectric [15]. Consequently, the high refractive index of the WO_3 layer could promote the extraction of the energy of the SPP modes from the front into the dielectric layer. The light reflected from the back reflector could become trapped again as SPP modes at the cathode surface. Therefore, the dielectric should be sufficiently thick to separate the light source and the cathode further apart than the near-field region. The results shown in Fig. 3 suggest that the 100 nm WO_3 was sufficiently thick to restrict near-field coupling in the path from the back reflector to the outside.

Conclusions

We investigated the light outcoupling enhancement method by extracting the light energy trapped in SPP modes. To extract the SPP mode energy, we used a multi-cathode structure composed of a thin cathode (Ag), a high refractive index dielectric layer (WO_3), and a reflector (Ag). The thicknesses of the Ag cathode and WO_3 dielectric were varied to examine the dependence of the current efficiency. The results demonstrated that current efficiency was improved more than 20% using this structure with an Ag cathode with a thickness of 50 nm and a WO_3 dielectric with a thickness of 100 nm.

Funding

This work was supported by the IT R&D program of MKE/KEIT (10041062, Development of fundamental technology for light extraction of OLED) and by the Soonchunhyang University Research Fund.

References

[1] Chutinan, A., Ishihara, K., Asano, T., Fujita, M., & Noda, S. (2005). *Org. Electron. 6*, 3.
[2] Nowy, S., Frischeisen, J., & Brütting, W. (2009). *Proc. of SPIE 7415*, 74151C.
[3] Meerheim, R., Nitsche, R., & Leo, K. (2008). *Appl. Phys. Lett. 93*, 043310.
[4] Cho, T.-Y., Lin, C.-L., & Wu, C.-C. (2006). *Appl. Phys. Lett. 88*, 111106.
[5] Do, Y. R., Kim, Y.-C., Song, Y.-W., & Lee, Y.-H. (2004). *J. Appl. Phys. 96*, 7629.
[6] Do, Y. R., Kim, Y. C., Song, Y.-W., Cho, C.-O., Jeon, H., Lee, Y.-J., Kim, S.-H., & Lee, Y.-H. (2003). *Adv. Mater. 15*, 1214.
[7] Moller, S., & Forrest, S. (2002), *J. Appl. Phys. 91*, 3324.

[8] Lin, H.-Y., Ho, Y.-H., Lee, J.-H., Chen, K.-Y., Fang, J.-H., Hsu, S.-C., Wei, M.-K., Lin, H.-Y., Tsai, J.-H., & Wu, T.-C. (2008). *Opt. Express 16*, 11044.
[9] Koh, T.-W., Choi, J.-M., Lee, S., & Yoo, S. (2010), *Adv. Mater. 22*, 1849.
[10] Bathelt, R., Buchhauser, D., & Gärditz, C. (2007). *Org. Electron. 8*, 293.
[11] Gifford, D. K., & Hall, D.G. (2002). *Appl. Phys. Lett. 81*, 4315.
[12] Wedge, S., Giannattasio, A., & Barnes, W.L. (2007), *Org. Electron. 8*, 136.
[13] Bi, Y.-G., Feng, J., Li, Y.-F., Jin, Y., Liu, Y.-F., Chen, Q.-D., & Sun, H.-B. (2012). *Appl. Phys. Lett. 100*, 053304.
[14] Mikami, A., & Goto, T. (2012). *SID Int. Symp. Dig. Tec. 43*, 683.
[15] Burke, J. J., Stegeman, G. I., & Tamir, T. (1986). *Phys. Rev. B 33*, 5186.
[16] Wedge, S., Hooper, I. R., Sage, I., & Barnes, W. L. (2004). *Phy. Rev. B 69*, 245418.
[17] Winter, G., & Barnes, W. L. (2006). *Appl. Phys. Lett. 88*, 051109.
[18] Liu, Z., Fang, N., Yen, T.-J., & Zhang, X. (2003). *Appl. Phys. Lett. 83*, 5184.
[19] Subrahmanyam, A., & Karuppasamy, A. (2007). *Sol. Energy Mater. Sol. Cells 91*, 266.